

## Kinetic Control of Chirality in Porphyrin J-Aggregates

Andrea Romeo,<sup>†,⊥</sup> Maria Angela Castriciano,<sup>\*,‡,⊥</sup> Ilaria Occhiuto,<sup>†</sup> Roberto Zagami,<sup>†</sup> Robert F. Pasternack,<sup>§</sup> and Luigi Monsù Scolaro<sup>\*,†,⊥</sup>

<sup>‡</sup>Istituto per lo Studio dei Materiali Nanostrutturati ISMN-CNR and <sup>†</sup>Dipartimento di Scienze Chimiche, University of Messina and CIRCMSB, 98166 Messina, Italy

<sup>§</sup>Department of Chemistry and Biochemistry, Swarthmore College, Swarthmore, Pennsylvania 19081, United States

### **S** Supporting Information

**ABSTRACT:** Detailed kinetic investigations demonstrate the fundamental role of kinetic parameters in the expression and transmission of chirality in supramolecular systems. The rate of the aggregation process leading to the formation of J-aggregates strongly affects the size of these nanoassemblies and the chiral induction.

Reports of optical activity for assemblies of achiral entities in the absence of templates were greeted at first with skepticism. However, now that these findings have been confirmed, considerable attention has been focused on this phenomenon. The possibility that what is being observed in these systems is a spontaneous mirror-symmetry breaking has led to speculation about the relationship of these processes to those responsible for the ubiquitous homochirality in our universe.<sup>1</sup> Some intriguing theories have been proposed for the putative role of external influences such as circularly polarized light,<sup>2–4</sup> electroweak interaction,<sup>5,6</sup> vortex motion,<sup>7,8</sup> stirring,<sup>8–19</sup> catalysis at prochiral crystal surfaces,<sup>20,21</sup> and combinations of external fields.<sup>22,23</sup> Alternatively, others have suggested that “hidden” templates such as trace impurities in solvents are responsible for the observed chirality.<sup>24</sup> All these experimental findings and speculations finally resolve on the question of how chirality is transferred from a chiral bias, either physical or chemical, to a growing assembly. Achiral chromophores, especially porphyrins, have been of some considerable importance for such symmetry-breaking studies due to their rich spectral properties and their ability (under appropriate conditions) to self-assemble into chiral supramolecular structures.<sup>25–30</sup> In particular, *meso*-4-sulfonatophenyl- and aryl-substituted porphyrins have been widely used as starting materials.<sup>31,32</sup> Recently, control of the handedness of chiral J-aggregates obtained from such achiral porphyrin monomers has been achieved by applying rotational, gravitational, and orienting forces at the beginning of the assembly process.<sup>23</sup> This experimental result underscores the role that even small, macroscopic chiral perturbations applied simultaneously with nucleation steps can have in directing the handedness of initially formed seeds, and thereby of the final supramolecular structure (“amplification effect”). The supramolecular aggregation processes are based on hierarchical self-assembly showing different thermodynamically and kinetically controlled paths related to medium properties and experimental conditions such as concentration, pH, and ionic

strength.<sup>25,33–35</sup> TPPS J-aggregates, obtained in aqueous solution in the absence of any added chiral templating agent, show an unpredictable chirality, resulting in controversial proposals for their basis. Since achiral monomers were used, it had been assumed that aggregates would be formed as a racemic mixture, exhibiting no optical activity.<sup>8</sup> When detected, TPPS J-aggregates’ optical activity had been proposed to arise through (among others) the adventitious presence of chiral impurities (i.e., “hidden” templates) or an intrinsically chiral arrangement of porphyrins in the unit cell.<sup>30</sup> In the presence of chiral templating reagents, such as tartaric acid, the situation might have been expected to be more straightforward, but kinetic investigations on the formation of J-aggregates of *meso*-tetrakis(4-sulfonatophenyl)porphyrin (TPPS) have shown distinct kinetic patterns and a corresponding variance in the amplification of chirality for the two enantiomers.<sup>25</sup>

In the current report, we attempt to resolve some of the confounding issues related to optical activity of assembly formation by providing an answer to a controversial question: Is there a correlation between the different methodologies used to initiate the aggregation and the rate constants for the process as well as the final observed optical activity? Here, we report on the kinetics of the self-assembly of TPPS in the absence of an added chiral template, investigated through a combination of UV/vis, circular dichroism (CD), and resonance light scattering (RLS) spectroscopies, and show that the supramolecular chirality is related to (i) reagent mixing protocol, (ii) kinetic rates, and (iii) aggregate size. The aggregation process was triggered in an aqueous solution by adding the porphyrin as first (PF) or last reagent (PL) (see Supporting Information (SI) for experimental details). The acidification of porphyrin solutions induces the self-assembling of the zwitterionic monomers (Soret band at 434 nm) into J-aggregated species characterized by an extinction band at 490 nm. Within these aggregates, the porphyrins are stacked side-by-side, are stabilized by electrostatic, hydrogen-bonding, and dispersive interactions,<sup>15,36–41</sup> and exhibit interesting exciton delocalization properties.<sup>42</sup>

Previous reports on porphyrin aggregation have pointed out the importance of establishing a well-defined protocol for reagent mixing in order to obtain reproducible results. This issue becomes particularly relevant when dealing with kinetic studies because the kinetics/mechanism of growth drive the

Received: October 14, 2013

Published: December 10, 2013

morphology of the resulting aggregates. If hydrochloric acid (0.5 M) is added to dilute porphyrin solution (3  $\mu\text{M}$ ) in PF protocol, the formation of the J-aggregated species follows a sigmoidal profile which is characterized by the presence of an induction period at the beginning of the process (Figure 1,

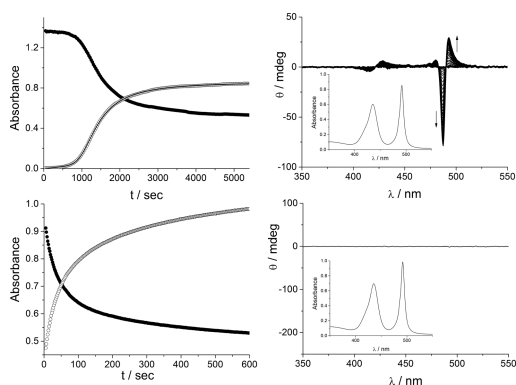


**Figure 1.** Extinction kinetic profiles and CD spectral changes for the aggregation of TPPS induced by HCl by using PF (upper) and PL (lower) protocols. The extinction spectra of J-aggregates are reported in the insets. [TPPS] = 3  $\mu\text{M}$ ; [HCl] = 0.5 M; for the kinetic plots,  $\lambda$  = 434 (full circles) or 491 nm (open circles);  $T$  = 298 K.

upper panel). The analysis of the kinetic traces has been performed through a nonconventional approach previously reported for porphyrin aggregation (eq 1 in the SI).<sup>43</sup> In such a model, the rate-determining step is the formation of a “critical size” assembly which catalyzes further growth.<sup>44–46</sup> As the aggregation continues, a positive bisignate induced Cotton effect, located at the aggregate absorption bands, appears in the CD spectra (Figure 1, upper panel), indicating chiral excitonic coupling of the chromophores in the self-assembly. If porphyrin is added as the last reagent (PL) to an acidic solution, a dramatic difference is observed in the kinetic profiles, which now obey a stretched exponential functional form (eq 2 in the SI), completely devoid of an initial induction time (Figure 1, lower panel). Somewhat surprising, when this protocol is used, while the UV/vis spectra remain almost unchanged from those obtained with the alternative protocol (insets of Figure 1), the CD spectrum shows a total absence of chirality induction in the aggregates region (Figure 1, lower panel) during the time course of the self-assembly process as well as 1 day later.

As previously reported, the CD signals for these J-aggregates cannot be attributed to artifacts due to linear dichroism.<sup>47</sup> In our case the reagent mixing order affects not only the kinetic rates of the self-assembly processes but also the induction of chirality in the supramolecular systems. To exercise kinetic control of the aggregation process and to explore its influence on the chirality, we investigated the formation of J-aggregates using the PF mixing order protocol, in which the nucleation stage could be easily monitored. As the aggregation process is clearly detectable in electronic and CD spectroscopies, both techniques were performed independently. The UV/vis and CD kinetic profiles are depicted in the upper panel of Figure 2. The two techniques show the same kinetic profile, indicating that chiral amplification, in the self-assembly of the achiral dyes, discloses the involvement of an autocatalytic pathway.

The sign and magnitude of the supramolecular chirality were further quantified by calculating the increase of the dissymmetry factor  $g$  ( $\Delta\epsilon/\epsilon$ ) as a function of time. This feature shows a biphasic behavior exhibiting a rapid increase in

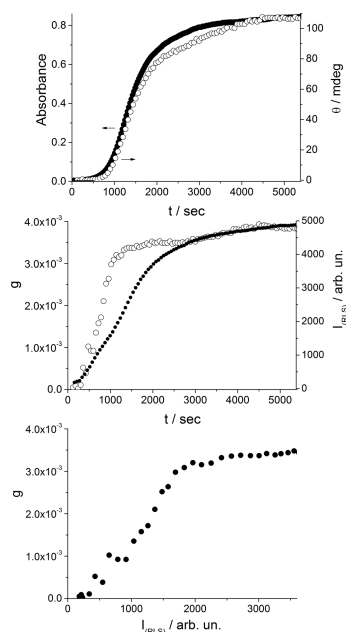


**Figure 2.** Absorption (full circle, upper panel) and CD (open circle, upper panel), RLS intensity (full circle, middle panel), and dissymmetry factor  $g$  (open circle, middle panel) kinetic profiles of TPPS aggregation induced by HCl using PF protocol. In the lower panel,  $g$  is reported as a function of RLS intensity. [TPPS] = 3  $\mu\text{M}$ ; [HCl] = 0.5 M;  $\lambda$  = 491 nm;  $T$  = 298 K.

a period corresponding roughly to the initial nucleation stage (accounting for  $\sim 80\%$  of the total effect), followed by a slower and smaller increase as aggregation proceeds, as probed by RLS measurements (Figure 2, middle panel). Since RLS intensity is very sensitive to the mean cluster size,<sup>48</sup> we estimated also the correlation between the size of the J-aggregates and their chirality by plotting the dissymmetry factor  $g$  with the intensity of the RLS during the kinetics of growth (Figure 2, lower panel). It is interesting to note that (i) the factor  $g$  increases linearly with the size of the J-aggregates, paralleling their growth, until a certain threshold size; above this size the factor  $g$  remains almost unchanged, exhibiting a much smaller dependence, likely due to structural disorder; (ii) the different rates for the increase of  $g$  and RLS intensity with time could suggest a somewhat different mechanism for optical activity with respect to the growth of the aggregates size; and (iii) the nucleation stage is of primary importance to chirality induction. All these findings point strongly to the conclusion that the observed chirality is a mesoscopic property of the growing supramolecular assembly and not a molecular one due only to a chiral building block.

To gain further insight into the effects exerted by the nucleation step, we performed a detailed kinetic investigation scanning a range of porphyrin concentrations from 1 to 10  $\mu\text{M}$ . The kinetic traces were analyzed using the aforementioned autocatalytic model.<sup>44,45</sup> The kinetic parameters are summarized in Table SII.

The values of the rate constants for the uncatalyzed pathway,  $k_0$ , and those for the catalyzed pathway,  $k_c$ , generally increase, with the latter exhibiting an exponential dependence on the initial porphyrin concentration (Figure 3, upper panel).  $k_0$  and  $k_c$  as well as  $m$  ( $\sim 2-4$ ), the critical size for the nuclei, and  $n$  ( $\sim 5-8$ ), the time exponent, are comparable to values reported in the literature for similar systems in aqueous solutions or in

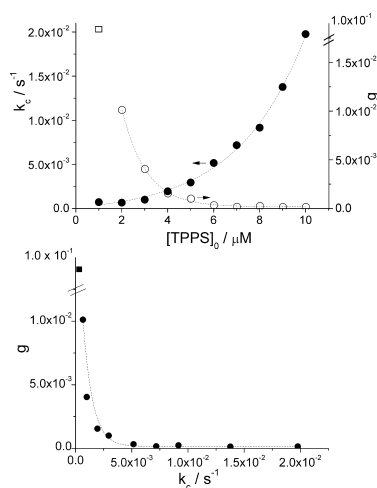


**Figure 3.** Plots of the kinetic rate constants  $k_c$  calculated by eq 1 (Supporting Information) and the factor  $g$  (upper panel) of the resulting chiral J-aggregates as functions of initial porphyrin concentration for the aggregation process using the PF protocol. In the lower panel  $g$  is reported as a function of the kinetic rate constants.  $[TPPS] = 1\text{--}10\ \mu\text{M}$ ;  $[\text{HCl}] = 0.5\ \text{M}$ ;  $T = 298\ \text{K}$ .

microemulsions.<sup>34,44,43</sup> CD spectra recorded at the end of the aggregation process show a positive bisignate Cotton effect centered at the aggregate absorption band (Figures SII–SI10). It is worth noting that the dissymmetry factor  $g$  decreases dramatically with increasing initial porphyrin concentration, i.e., with increase of the aggregation rate (Figure 3, upper and lower panels). Indeed, at high porphyrin concentration ( $>10\ \mu\text{M}$ , see Figure SII1) the CD signal is virtually undetectable, even for the PF protocol. Thus, both the values of the experimental kinetic parameters and the dissymmetry factors  $g$  prove to be highly sensitive not only to the mixing protocol but also to relatively small differences in initial dye concentrations.<sup>49</sup> Our findings point to the important role of the nucleation stage preceding the growth of the final assemblies: when a large number of seeds are formed very quickly, as in the PL protocol, or by increasing either the concentration of porphyrin or the ionic strength in the PF protocol,<sup>50,51</sup> no CD band is detected for the samples. Using the PF protocol, the nucleation period shortens upon increasing the porphyrin concentration (Figures SII–SI10), and the measured  $m$  values imply that the rate of the aggregation process and consequently the expression of chirality are very sensitive to even small oligomers (dimers or trimers). Interestingly, the average  $m$  value, i.e., the size of the critical nucleus, observed in our experiments ( $\sim 3$ ) is the same as the value suggested by Ribò et al. using spectroscopic measurements on a closely related system.<sup>19</sup>

Moreover, the intensity of the RLS, corrected for the concentration of porphyrin as part of the aggregates (as extinction of the samples), exhibits a nonlinear decrease on increasing the initial dye concentration (Figure 4, left panel). Given that the intensity of scattered light is an indirect measure of the aggregate size, this evidence suggests that, on increasing the porphyrin concentration, the aggregation rate increases and the size of the final aggregates decreases. These results are consistent with previous observations,<sup>33</sup> which can now be explained as due to rapid nucleation preceding the growth of ordered structures. On increasing the concentration of the reagents, a larger number of initial nuclei are quickly formed, leading to aggregates of smaller sizes.<sup>52</sup> Figure 4 (right panel)

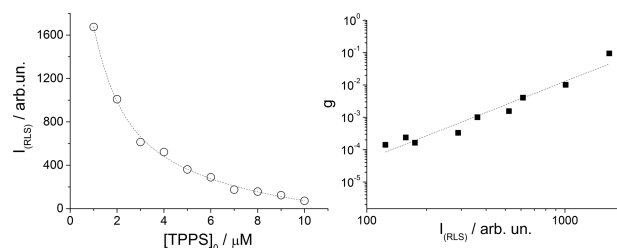


**Figure 4.** Plot of final RLS intensity corrected for absorption as a function of the initial porphyrin concentration (left panel) and double logarithm plot of the factor  $g$  vs the corrected final RLS intensity (right panel).  $[\text{HCl}] = 0.5\ \text{M}$ ;  $T = 298\ \text{K}$ .

shows that the values of the  $g$  factor as a function of the corresponding intensity of the RLS, i.e., the size of the aggregates, obey a scaling law of the type  $g \propto I_{\text{RLS}}^\beta$  ( $\beta = 2.4 \pm 0.2$ ,  $R^2 = 0.98$ ). This observation suggests that, similar to what is observed in a confined environment,<sup>26</sup> (i) a very efficient mechanism for the chirality propagation is operating within these aggregates, and (ii) the dissymmetry factor  $g$  decreases as the rate of aggregation increases.

In conclusion our results strongly suggest that, whatever the source of the chiral bias promoting symmetry breaking, the rate of the aggregation process leading to the formation of J-aggregates strongly affects the size of these nanoassemblies and the chiral induction. Whether the observed nulling effect on electronic CD spectra is due to an effective racemization upon increasing the aggregation rates or to a lower efficiency in transmitting chirality in small nanoaggregates<sup>26</sup> is still an open question. These data provide an explanation for the apparent discrepancy in the literature as to the chirality observed using very different initial conditions. To the best of our knowledge, this report represents the first detailed kinetic investigation, in an aqueous solution, to demonstrate the fundamental role of kinetic parameters in the expression and transmission of chirality in supramolecular systems.

## ■ ASSOCIATED CONTENT

### 📄 Supporting Information

Experimental details; kinetic parameters, profiles, and final spectra at different porphyrin concentrations; CD spectrum of TPPS J-aggregates at different experimental conditions. This material is available free of charge via the Internet at <http://pubs.acs.org>.

## ■ AUTHOR INFORMATION

### Corresponding Authors

castriciano@pa.ismnr.it  
lmonsu@unime.it

### Author Contributions

<sup>†</sup>A.R., M.A.C., and L.M.S. contributed equally.

### Notes

The authors declare no competing financial interest.

## ■ ACKNOWLEDGMENTS

The authors thank MIUR (PRIN 2010–2011 project no. 2010C4RM8), CNR, for financial support and Mr. G. Irrera (CNR-ISMN) for technical assistance.

## ■ REFERENCES

(1) Wagnière, G. H. *On Chirality and the Universal Asymmetry: Reflections on Image and Mirror Image*; Wiley-VCH: Weinheim, 2007.

- (2) Bailey, J.; Chrysostomou, A.; Hough, J. H.; Gledhill, T. M.; McCall, A.; Clark, S.; Ménard, F.; Tamura, M. *Science* **1998**, *281*, 672.
- (3) Flores, J. J.; Bonner, W. A.; Massey, G. A. *J. Am. Chem. Soc.* **1977**, *99*, 3622.
- (4) Noorduyn, W. L.; Bode, A. A. C.; van der Meijden, M.; Meekes, H.; van Etteger, A. F.; van Enckevort, W. J. P.; Christianen, P. C. M.; Kaptein, B.; Kellogg, R. M.; Rasing, T.; Vlieg, E. *Nat. Chem.* **2009**, *1*, 729.
- (5) Kondepudi, D. K.; Nelson, G. W. *Nature* **1985**, *314*, 438.
- (6) Berger, R.; Quack, M. *ChemPhysChem* **2000**, *1*, 57.
- (7) Aquilanti, V.; Maciel, G. S. *Orig. Life Evol. Biosph.* **2006**, *36*, 435.
- (8) D'Urso, A.; Randazzo, R.; Lo Faro, L.; Purrello, R. *Angew. Chem., Int. Ed.* **2010**, *49*, 108.
- (9) Jacques, J.; Collet, A.; Wilen, S. H. *Enantiomers, Racemates, and Resolutions*; Krieger Publishing Co.: Malabar, FL, 1994.
- (10) Kondepudi, D. K.; Kaufman, R. J.; Singh, N. *Science* **1990**, *250*, 975.
- (11) Kondepudi, K.; Bullock, K. L.; Digits, J. A.; Hall, J. K.; Miller, J. M. *J. Am. Chem. Soc.* **1993**, *115*, 10211.
- (12) Kondepudi, D. K.; Laudadio, J.; Asakura, K. *J. Am. Chem. Soc.* **1999**, *121*, 1448.
- (13) Link, D. R.; Natale, G.; Shao, R.; MacLennan, J. E.; Clark, N. A.; Körblová, E.; Walba, D. M. *Science* **1997**, *278*, 1924.
- (14) Huang, X.; Jiang, C. Li.S.; Wang, X.; Zhang, B.; Liu, M. *J. Am. Chem. Soc.* **2004**, *126*, 1322.
- (15) Ribo, J. M.; Crusats, J.; Sagues, F.; Claret, J.; Rubires, R. *Science* **2001**, *292*, 2063.
- (16) Ribó, J. M.; Bofill, J. M.; Crusats, J.; Rubires, R. *Chem.—Eur. J.* **2001**, *7*, 2733.
- (17) Escudero, C.; Crusats, J.; Díez-Pérez, I.; El-Hachemi, Z.; Ribó, J. M. *Angew. Chem., Int. Ed.* **2006**, *45*, 8032.
- (18) Arteaga, O.; Canillas, A.; Crusats, J.; El-Hachemi, Z.; Llorens, J.; Sacristan, E.; Ribo, J. M. *ChemPhysChem* **2010**, *11*, 3511.
- (19) Sorrenti, A.; El-Hachemi, Z.; Crusats, J.; Ribo, J. M. *Chem. Commun.* **2011**, *47*, 8551.
- (20) Kuhn, A.; Fischer, P. *Angew. Chem., Int. Ed.* **2009**, *48*, 6857.
- (21) Kawasaki, T.; Kamimura, S.; Amihara, A.; Suzuki, K.; Soai, K. *Angew. Chem., Int. Ed.* **2011**, *50*, 6796.
- (22) Rikken, G. L. J. A.; Raupach, E. *Nature* **2000**, *405*, 932.
- (23) Micali, N.; Engelkamp, H.; van Rhee, P. G.; Christianen, P. C. M.; Scolaro, L. M.; Maan, J. C. *Nat. Chem.* **2012**, *4*, 201.
- (24) El-Hachemi, Z.; Escudero, C.; Arteaga, O.; Canillas, A.; Crusats, J.; Mancini, G.; Purrello, R.; Sorrenti, A.; D'Urso, A.; Ribo, J. M. *Chirality* **2009**, *21*, 408.
- (25) Castriciano, M. A.; Romeo, A.; Zagami, R.; Micali, N.; Scolaro, L. M. *Chem. Commun.* **2012**, *48*, 4872.
- (26) Castriciano, M. A.; Romeo, A.; De Luca, G.; Villari, V.; Scolaro, L. M.; Micali, N. *J. Am. Chem. Soc.* **2011**, *133*, 765.
- (27) van Hameren, R.; van Buul, A. M.; Castriciano, M. A.; Villari, V.; Micali, N.; Schoen, P.; Speller, S.; Scolaro, L. M.; Rowan, A. E.; Elemans, J. A. A. W.; Nolte, R. J. M. *Nano Lett.* **2008**, *8*, 253.
- (28) Scolaro, L. M.; Castriciano, M. A.; Romeo, A.; Micali, N.; Angelini, N.; Lo Passo, C.; Felici, F. *J. Am. Chem. Soc.* **2006**, *128*, 7446.
- (29) Short, J. M.; Berriman, J. A.; Kübel, C.; El-Hachemi, Z.; Naubron, J.-V.; Balaban, T. S. *ChemPhysChem* **2013**, *14*, 3209.
- (30) El-Hachemi, Z.; Escudero, C.; Acosta-Reyes, F.; Casas, M. T.; Altoe, V.; Aloni, S.; Oncins, G.; Sorrenti, A.; Crusats, J.; Campos, J. L.; Ribo, J. M. *J. Mater. Chem. C* **2013**, *1*, 3337.
- (31) Schwab, A. D.; Smith, D. E.; Rich, C. S.; Young, E. R.; Smith, W. F.; de Paula, J. C. *J. Phys. Chem. B* **2003**, *107*, 11339.
- (32) Collini, E.; Ferrante, C.; Bozio, R. *J. Phys. Chem. B* **2005**, *109*, 2.
- (33) Micali, N.; Villari, V.; Castriciano, M. A.; Romeo, A.; Scolaro, L. M. *J. Phys. Chem. B* **2006**, *110*, 8289.
- (34) Castriciano, M.; Romeo, A.; Villari, V.; Micali, N.; Scolaro, L. M. *J. Phys. Chem. B* **2003**, *107*, 8765.
- (35) Besenius, P.; Portale, G.; Bomans, P. H. H.; Janssen, H. M.; Palmans, A. R. A.; Meijer, E. W. *Proc. Natl. Acad. Sci. U.S.A.* **2010**, *107*, 17888.
- (36) Gandini, S. C. M.; Gelamo, E. L.; Itri, R.; Tabak, M. *Biophys. J.* **2003**, *85*, 1259.
- (37) Collings, P. J.; Gibbs, E. J.; Starr, T. E.; Vafek, O.; Yee, C.; Pomerance, L. A.; Pasternack, R. F. *J. Phys. Chem. B* **1999**, *103*, 8474.
- (38) Akins, D. L.; Ozcelik, S.; Zhu, H. R.; Guo, C. *J. Phys. Chem.* **1996**, *100*, 14390.
- (39) Ribo, J.; Crusats, J.; Farrera, J.; Valero, M. *J. Chem. Soc., Chem. Commun.* **1994**, 681.
- (40) Pasternack, R. F.; Schaefer, K. F.; Hambright, P. *Inorg. Chem.* **1994**, *33*, 2062.
- (41) Ohno, O.; Kaizu, Y.; Kobayashi, H. *J. Chem. Phys.* **1993**, *99*, 4128.
- (42) Salomon, A.; Wang, S. J.; Hutchison, J. A.; Genet, C.; Ebbesen, T. W. *ChemPhysChem* **2013**, *14*, 1882.
- (43) Castriciano, M. A.; Romeo, A.; Villari, V.; Micali, N.; Scolaro, L. M. *J. Phys. Chem. B* **2004**, *108*, 9054.
- (44) Pasternack, R. F.; Fleming, C.; Herring, S.; Collings, P. J.; dePaula, J.; DeCastro, G.; Gibbs, E. J. *Biophys. J.* **2000**, *79*, 550.
- (45) Pasternack, R. F.; Gibbs, E. J.; Collings, P. J.; dePaula, J. C.; Turzo, L. C.; Terracina, A. *J. Am. Chem. Soc.* **1998**, *120*, 5873.
- (46) Balaban, T. S.; Leitich, J.; Holzwarth, A. R.; Schaffner, K. *J. Phys. Chem. B* **2000**, *104*, 1362.
- (47) Sorrenti, A.; El-Hachemi, Z.; Arteaga, O.; Canillas, A.; Crusats, J.; Ribo, J. M. *Chem.—Eur. J.* **2012**, *18*, 8820.
- (48) Micali, N.; Monsu' Scolaro, L.; Romeo, A.; Mallamace, F. *Phys. Rev. E* **1998**, *57*, 5766.
- (49) As the nature of the counteranion could influence the structure of the final aggregates, we performed the same experiments using H<sub>2</sub>SO<sub>4</sub> acid instead of HCl to trigger the aggregation process. Both the catalytic kinetic rate constants and the corresponding dissymmetry factor values show the same behavior for H<sub>2</sub>SO<sub>4</sub> as for HCl.
- (50) When the experimental conditions reported by Purrello et al.<sup>8</sup> are used, no chirality is detected, in line with very fast nucleation and aggregation kinetics (see Figure SI13).
- (51) The effect of aggregation rates on the induction of optical activity has been further supported by slowing down the kinetics through an increase in the pH: using a 10 μM TPPS solution, where no or very low signals are usually detectable at [HCl] = 0.5 M, a clear signal could be observed when [HCl] = 0.08 M (see Figure SI12).
- (52) Burda, C.; Chen, X.; Narayanan, R.; El-Sayed, M. A. *Chem. Rev.* **2005**, *105*, 1025.